https://doi.org/10.2352/ISSN.2470-1173.2021.5.MAAP-132

Next Best Light Position: A self configuring approach for the Reflectance Transformation Imaging acquisition process

Ramamoorthy Luxman [a], ***Marvin Nurit*** [b], ***Gaëtan Le Goïc*** [c], ***Franck Marzani*** [d], ***Alamin Mansouri*** [e]
ImViA Laboratory (EA 7535), Université Bourgogne Franche-Comté (UBFC), Dijon, France

Abstract

Reflectance Transformation Imaging (RTI) is a computational photographic method that captures an object's surface shape & color and enables the interactive re-lighting of the subject from any direction. RTI model of an object is built from multiple images of it captured by a stationary camera but varying light directions. By changing the direction of the light, the respective micro-geometry of the object is highlighted. The RTI acquisition process is often long, and tedious when it is not automated. It requires expertise to define for each analysed object which are the number and the relevant lighting positions in the acquisition sequence. In this paper, we present our novel Next Best Light Position (NBLP) method to address this issue. The proposed method is based on the principle of a gradient descent allowing in an adaptive and iterative way, to automatically define the most appropriate lighting directions for the RTI acquisition of an object/surface.

Introduction

RTI is one of the widely used imaging techniques for cultural heritage objects [2].The two most popular methods adopted for performing the RTI acquisitions[1] are: 1. Using a handheld light source and manually illuminating the stationary object from different directions while the camera is fixed on a stationary tripod [4]. This is known as highlight RTI (H-RTI). This method is suitable for objects that are bigger in size and where there is no access to sophisticated systems and equipment. 2. Hemispherical lighting dome (see figure 1a having lights positioned in fixed directions or has an internal mechanism that moves the light source from one point to another (figure 1b). The camera is fixed at the apex of the hemispherical dome and is triggered in synchronization with the lighting. The dome system is usually adopted in a laboratory environment where it is highly calibrated and built upon an optical table. This set up is suitable for performing the RTI acquisition of smaller objects. In both cases, it is important to formulate a strategy for positioning the light for each image capture during the acquisition to ensure good results. In H-RTI, commonly, one or more reflective spheres are used to determine the light directions. This is a more cost-effective practice to recover light directions than a fully calibrated acquisition system which are generally expensive.

The overall objective of this work is to formulate a strategy to estimate the next best light positions from an initial set of images captured during RTI acquisitions. The idea is a direct offshoot of the desire to ensure that all the critical light directions of the surface are captured in an acquisition, to decrease the number of images captured during an RTI acquisition and thereby reduce the overall acquisition time, and to realize the possibility of automating the acquisition. Indeed, in a RTI acquisition where the light positions are chosen intuitively or set uniformly around the object, not all the important light directions are captured and conversely all captured images often do not contribute significantly in the RTI model. For example, at a grazing angle, the reflection of a relatively flat surface is often close to zero, and at positions normal the pixel intensities attain saturation. Having too many images with zero or saturated pixel intensities, which are actually non-measured information's, is not desirable as these images are not useful, and can even be detrimental for the RTI model quality. For certain application domains, such as Cultural Heritage or industrial ones, it is also of primary importance to optimize the acquisition time. Indeed, access to CH objects for acquisition is often limited to a short period of time, and the industrial context often makes the cycle time determining in the choice of a technology. In cases similar to this, it is thus very important to perform good quality acquisition, in a single attempt.

The NBLP approach aims to adaptively measure the strictly necessary information according to the object analyzed. This approach determine automatically the appropriate light positions for RTI acquisition. Our method is an iterative and adaptive approach that estimates the next best light positions during the RTI acquisition process non-stochastically. We conceived the acronym NBLP for RTI scanning in analogous to NBV (Next Best View) for 3D scanning [3]. The proposed method have been implemented in the existing RTI dome system presented in figure 1a and 1b. We show the advantages of the implemented method by comparing the acquisition made with the NBLP determined light positions to that made with predefined light positions. We evaluate the performance of our proposed method using the histogram of mean pixel intensities of the images captured, finding the closeness of the results to that of a dense acquisition and finally by comparing the gradient fields. In addition to the presented method, in this paper we also briefly discuss our experience with a few other approaches and the reasons why they fail to yield the desired results.

(a) Inhouse RTI dome system (b) Mechanised light source

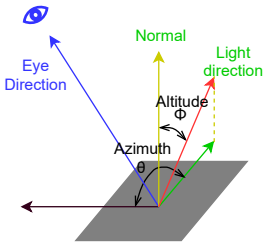

$$N \equiv \frac{\partial^2 P}{\cos\Theta \partial A \partial \Omega} [W \cdot cm^{-2} \cdot sr^{-1}] \ldots \quad (1)$$

Figure 2: Bidirectional Reflectance Distribution Function (BRDF)

State of the art

The reflectance of the surface of an opaque body is a property of the surface material and of its microscopic configuration (roughness) but also of its gross configuration (curvature) [5]. Bidirectional reflectance can be determined as a function of light direction as illustrated in figure 2. For example, in a perfect mirror, the distribution of reflected light direction is the same as the viewers direction, while in the case of a diffused surface the the distribution is uniform in all directions.The Reflectance Transformation Imaging technique is a partial BRDF where the observer is fixed, generally orthogonally to the surface to be inspected, and only the lighting direction varies in the acquisition sequence. The discrete angular reflectance is thus estimated in the directions of acquisition. An experimental model can then be determined by both Least square fitting (global approximation), local approximation or interpolation approaches. The main used global approximation model used in the case of RTI data are the Polynomial Texture Mapping approach (PTM) [1], the Hemispherical Harmonics (HSH) [6, 7], and the Discrete Modal Decomposition (DMD) [8]. These techniques are becoming widely used among the cultural heritage conservators as well as in industry for the control of the appearance on manufactured surfaces.

According to best of the authors knowledge there are no standard method to estimate salient light directions during the RTI acquisition process. The light positions are predetermined either homogeneously over the surface of the object or points defined by certain patterns. Both the size and configuration of acquisitions are determined empirically involving multiple attempts and hence the acquisition remains a tedious and time consuming process. Making a continuous acquisition instead of discrete light directions eliminates the problem of choosing the salient light directions. However continuous acquisition from every possible light direction is not practically feasible and the size of the data will be too big to handle. Multi-modal acquisition like multi-spectral [10], high dynamic range RTI [11], UV are the growing trends in RTI where enormous data is generated during acquisition and hence continuous acquisition poses numerical practical problems. Besides, cultural heritage conservation, RTI is oftentimes applied in industries too as a tool for engineering failure analysis [12], [13]. Automation of RTI acquisition using robot arm is another domain that draws much interest from the RTI users community as that will be an efficient way of performing the acquisitions in terms of both quality and time. NBLP is an important step towards enabling a fully automated pipeline for performing the reflectance transformation imaging. The closest analogy to NBLP is the NBV problem where it is desired to estimate a good sequence of range-image views during the scanning process for obtaining the complete 3D model of an object or scene.

NBLP-RTI acquisition strategy

In this section, we present our approach to the NBLP problem running through the development iterations. We describe our initial approaches that didn't yield the desired results along with their drawbacks first and then the working method is explained.

Method based on finding the local disparity among the images captured from neighbouring light positions

Fig. 3 represent the schematic of this method. This method is backed by the idea that more an image is different from those captured with neighbouring LPs, more are the chances that significant surface details can be captured between these neighbouring LPs. This method was implemented using K-D tree to find the neighbourhoods. The drawback of this approach is that it is very sensitive to the initial set of LPs. Through the iterations, it fails to expand globally and tends to get trapped within a few neighborhood that has the highest disparity. Thus, this method may be useful as a last step to verify whether all the salient directions are captured or not in a dense acquisition but is not suitable as a fully automated adaptive acquisition method.

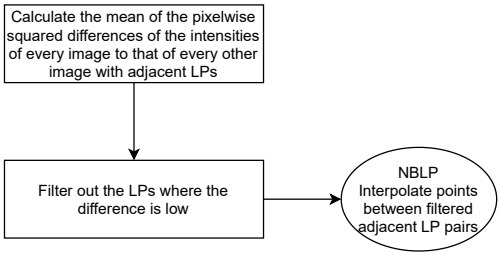

Figure 3: Method based on finding the local disparity among the images captured from neighbouring light positions

Method based on gradient ascent

In this approach, an initial sparse acquisition is made by illuminating the surface from directions homogeneously distributed around it. For the acquired images and light positions, model fitting of the pixel intensities are carried out individually against the spherical co-ordinates of the light positions. Gradient vector field of the fitted model and its steepest ascent direction is computed for each pixel. Weights are assigned to pixels proportional to its variance and a global steepest ascent direction is estimated as the weighted mean of the local steepest ascents. This global ascent is regarded as the next best light direction. This method is computationally very expensive and is practically challenging to execute during the acquisition process.

Method based on interpolation of points between salient LP pairs

The flow chart in Fig. 4 illustrates this approach to estimating the next best light positions during an acquisition.

For a good comparison of this approach to the existing practice, we have chosen an Egyptian currency coin Fig. 5 (S1) with high degree of surface details and a highly polished metallic surface Fig. 6 (S2) as the subjects . S1 is feature-rich surface profile where as S2 is polished and is more like a mirror. Our method is

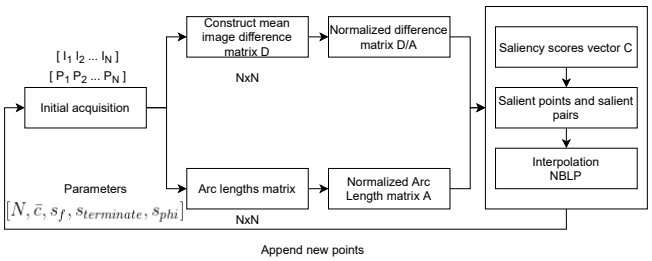

Figure 4: Schematic of the implemented NBLP method.

compared with the acquisitions made with uniformly distributed light positions.

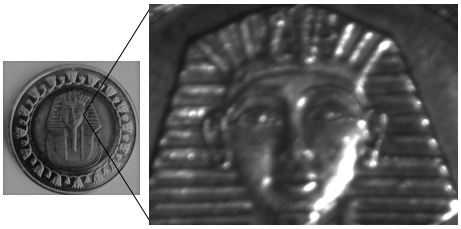

Figure 5: S1 surface acquired for comparison of results

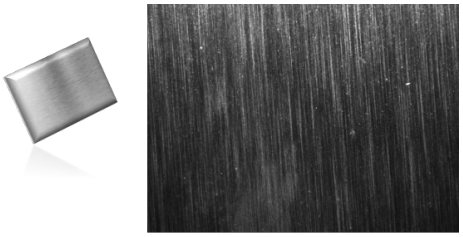

Figure 6: S2 surface acquired for comparison of results

Similar to our previous approach, an initial sparse acquisition (Eq.2) is made by capturing images with N number of homogeneously distributed light positions. A set of next best light positions are estimated from this initial acquisition consisting of N images, I taken with N difference light directions, P (θ, ϕ).

$$Acq = \begin{cases} I_1 & I_2 & I_3 & ... & I_N \\ P_1 & P_2 & P_3 & ... & P_N \end{cases} \tag{2}$$

A score function C_i representing the highest deviation of an image from the other images is defined to assign the salience of the corresponding pair of light directions. This function is as given below in Eq. 3 - 5

$$C_i = max\left(\frac{{}^i_1\mathrm{D}}{{}^i_1\mathrm{A}}, \frac{{}^i_2\mathrm{D}}{{}^i_2\mathrm{A}}, \frac{{}^i_3\mathrm{D}}{{}^i_3\mathrm{A}}, ..., \frac{{}^i_N\mathrm{D}}{{}^i_N\mathrm{A}}\right) \tag{3}$$

$${}^i_j\mathrm{D} = \frac{I_i - I_j}{size(I)} \tag{4}$$

$$\begin{aligned} {}^i_j\mathrm{A} = arccos[&(sin(\Phi_i) \times sin(\Phi_j)) \\ &+ (cos(\Phi_i) \times cos(\Phi_j) \times cos(\Theta_i - \Theta_j))] \end{aligned} \tag{5}$$

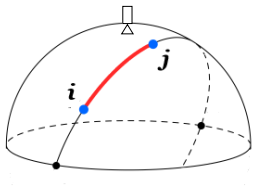

Figure 7: Arc distance between light directions i and j.

Here, ${}^j_i\mathrm{D}$ is the mean value of the difference between image i and image j, ${}^i_j\mathrm{A}$ is the relative arc distance between light positions i and j along the hemisphere, $size(I)$ is the total number of pixels in the image , θ_i and ϕ_i represents the azimuth and altitude of the light position i. The salience score C_i, is a measure of the gradient at the light position i and a higher score would indicate a higher possibility of capturing relatively more significant detail that between the i light position and its salient pair.

The salience scores of the LPs are then normalized between 0 to 1 for conveniently scaling and filtering. The LPs are identified as critical LP and non-critical LP based on their respective salience scores. The LPs having scores lesser than a threshold score, $\bar{c}$ are considered non-critical directions and the LPs having score higher than the threshold are considered as critical directions as shown in the Eq. 6

$$\begin{aligned} Acq_{critical} &\subset Acq \\ P_{critical} &= \{P : C > \bar{c}\} \end{aligned} \tag{6}$$

After identifying the critical light directions, a new set of light directions are determined by linearly interpolating points between every salient direction and its corresponding salient pair. This interpolation is carried out along the hemispherical arc between the pair. The number of interpolation points between a pair of directions is set as proportional to the salience score by multiplying the score with a constant called interpolation scale factor, s_f

This is illustrated with a critical point P_1 and its critical pair P_3 in the coin acquisition as an example in the Fig. 8

The new set of captures is appended to the initial acquisition and the whole process is repeated with the appended set as the current state of the acquisition. The iteration terminates when 1. the highest of ${}^i_jD$ of all the critical pairs is lower than a threshold intensity called $i_{terminate}$ or 2. all the estimated new LPs are already acquired in the previous iterations.

The size of the acquisition, the behaviour of the implemented NBLP algorithm can be tuned by adjusting the following parameters.

Parameter	Description	Range
N	Size of the initial acquisition	Ideally 30 to 45
$\bar{c}$	Minimum salience score threhold	[0, 1]
s_f	Interpolation scale factor	>0
$i_{terminate}$	Threshold intensity for termination	[0, 255]
s_{phi}	Phi scale factor to force interpolation along azimuth	[0, 1]

Results and discussions

The next best light position estimation algorithm based on interpolation of points between salient LP pairs is successfully implemented and integrated to our in house RTI acquisition software. Our approach is able to identify the critical directions as

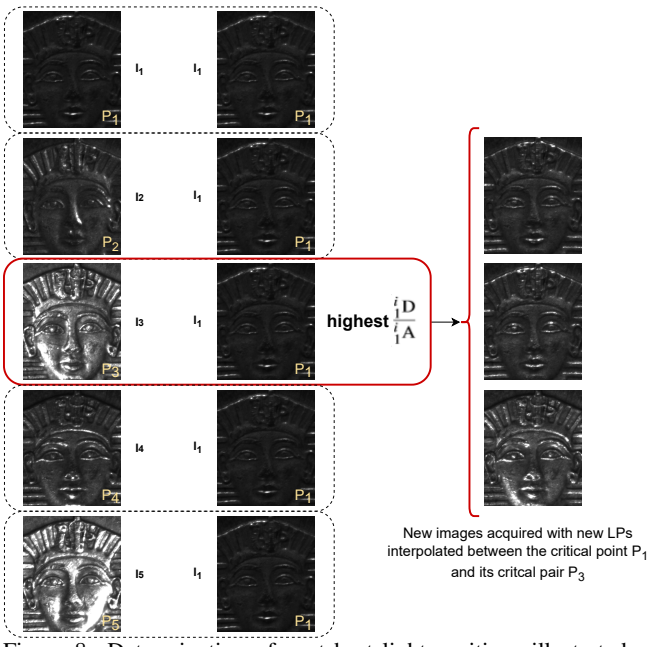

Figure 8: Determination of next best light positions illustrated with critical point P_1 and its critical pair P_3 as an example.

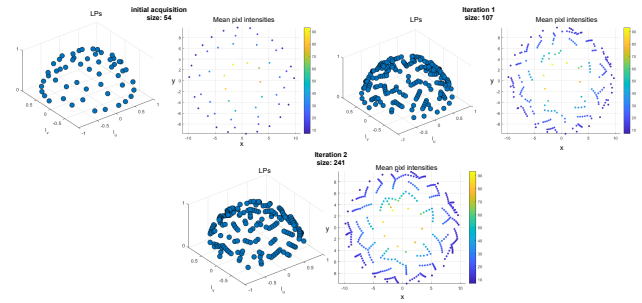

(a) Surface S1

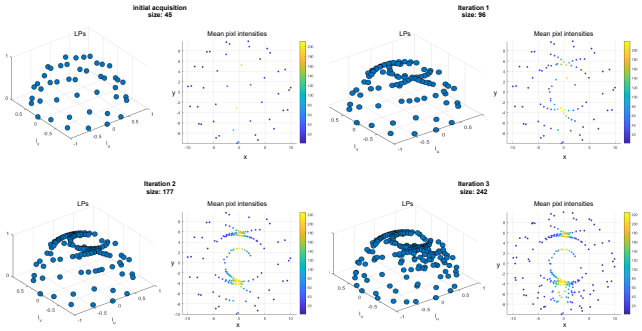

(b) Surface S2

Figure 9: Acquisitions of S1 and S2 surfaces evolving through the NBLP iterations.

the acquisition process progresses and thus the acquisition evolves emphasising the identified critical light directions. The approach is tested with different surfaces and in this paper to demonstrate the performance of NBLP over the common approach we present the results of the acquisitions carried out for surfaces S1 and S2.

Fig 9 shows the evolving of the acquisitions made with the implemented NBLP algorithm. In each iteration, the plots on the left represents the light positions in the 3D hemisphere and the plots on the right represents mean pixel intensities of the image captured at each light positions projected on a 2D plane. The scale in the plot is the color scale indicating the pixel intensities ranging from 0 to 255. S1 surface acquisition Fig. 9a terminated after 3 iterations. For this acquisition the parameters are set as number of $N = 54$, $\bar{c} = 0.75$, $s_f = 50.0$, $i_{terminate} = 2.5$, $s_{phi} = 0.75$. It can be observed that, the surface being a diffused surface, the reflectance is nearly uniform along all the directions. NBLP identifies majority of the directions as critical direction as the reflectance changes at uniform rate along θ and ϕ. As a result, the NBLP estimated light positions exhibits an artifact like patterns for this surface. Fig. 9b shows the evolving of S2 surface acquisition. This surface the acquisition terminated after 4 iterations. For this acquisition the parameters are set as number of $N = 45$, $\bar{c} = 0.75$, $s_f = 12.0$, $i_{terminate} = 5.0$, $s_{phi} = 0.75$. s_f is set lower for this surface because the overall reflectance of this surface is higher. Unlike in case of S1, it can be observed from the plots that the NBLP method identified specific light directions such as x{-3, 2} in the plot as the most critical light directions and tried to capture images densely along these directions.

Fig. 10 compares the end results of the homogeneous vs the NBLP acquisitions for S1 surface (Fig. 10a, Fig. 10b) and for S2 surface (Fig. 10c, Fig. 10d). S1 surface acquisition terminated after capturing images from 421 number of unique light directions. S2 surface acquisition terminated after capturing images from 242 number of unique light directions. For analysing the performance of the NBLP method, the homogeneous acquisition is made close to the size of the NBLP acquisition. From these plots, it is observed that the light directions where the reflection is very high (orange) and the light directions where the reflection is low (blue) are captured but the intermediary light directions are mostly not captured in case of the homogeneous acquisition. Where as in the NBLP acquisition, it is observed that intermediary light directions (from blue, red to orange, yellow) are well captured.

Fig. 11 are the histogram plots of the acquisition of S1 and S2 surfaces. The homogeneous acquisition (red) and the NBLP acquisition (blue) histograms are plotted overlapping each other for easy comparison. In the histogram plot, it can be clearly inferred that in case of homogenous acquisition, there are many insignificant light directions captured. For example, there are number of images captured from the light directions where the reflectance is nearly 0. These images carry insignificant surface information. On the contrary, the NBLP clearly avoided more number of captures on these directions and tried to acquire as dense as possible along the light directions where the reflectance is unique and carry significant surface information.

From the acquired images and the respective light directions, relighting model of the surfaces were performed using DMD method. Fig. 12 shows a directional slope of the reconstructed surface model for comparing the results of the homogeneous acquisition and NBLP acquisition. It is observed that for S1 surface, the visible difference between the reconstructed surfaces is low. Where the difference is easily visible in case of S2 surface. The dark pixels visible on the upper part of the rebuilt surface represents the lack of information that the homogeneous acquisition missed to capture.

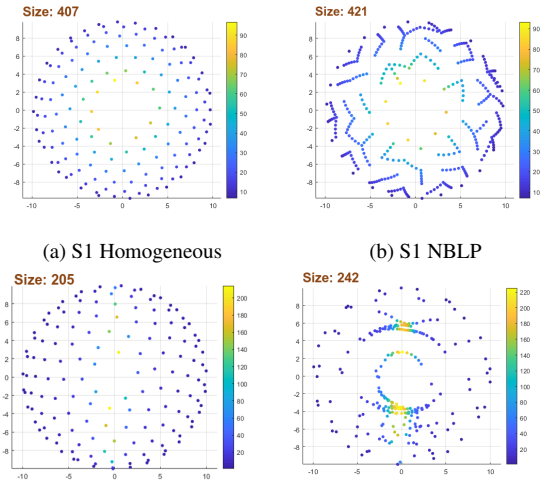

(a) S1 Homogeneous (b) S1 NBLP

(c) S2 Homogeneous (d) S2 NBLP

Figure 10: Comparison of acquisitions made with the predetermined homogeneously distributed light directions vs NBLP esimtated light directions.

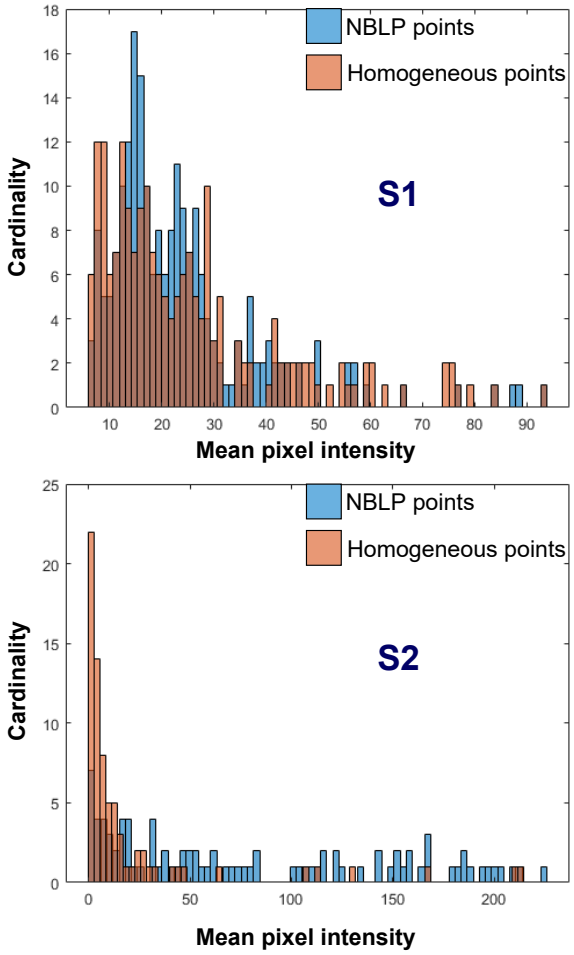

Figure 11: Histograms of the mean pixel intensities of the images captured in homogeneous acquisition and NBLP acquisitions.

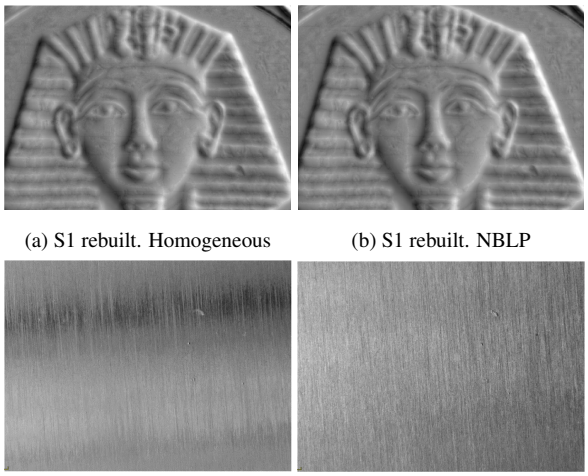

(a) S1 rebuilt. Homogeneous (b) S1 rebuilt. NBLP

(c) S2 rebuilt. Homogeneous (d) S2 rebuilt. NBLP

Figure 12: Surface reconstructed (directional slopes) from the homogeneous LPs acquisition vs the NBLP acquisition data using the DMD RTI model.

Conclusions

We recognised the importance and advantages of identifying relevant light directions in an acquisition and the same is explained in this paper. There are no existing work published that addresses this problem for RTI. We proposed our novel approach to estimate the best light positions for building the reflectance model of a surface. Our method is adaptive to the surface being scanned and automatically detects the critical directions as the acquisition evolves and tries to acquire dense information in those directions. Whereas the commonly applied homogeneous light positions approach the scan configurations are prefixed regardless of the surface being scanned. We have demonstrated the performance of our algorithm comparing with that of standard homogeneous acquisition. The mean pixel intensities plot, histogram plots, the reconstructed images illustrates the significance of using the NBLP approach over the standard predetermined light positions approach. It can be observed that our method tends to form artifacts like arcs and patterns. This is because of linear interpolation points between the critical point and its critical pair.

Our method is a first step toward the adaptive RTI acquisition. This is particularly useful for multi-modal RTI acquisitions like multi spectral or High Dynamic RTI in the sense that it allows to measure just necessary information.

Acknowledgement

This work has received funding from the European Union's Horizon 2020 research and innovation program under the Marie Skłodowska-Curie grant agreement No. 813789.

References

[1] Malzbender, Tom and Gelb, Dan and Wolters, Polynomial texture maps, Proc. 28th annual conference on Computer graphics and interactive techniques, pages 519-528, 2001

[2] Castro, Yuly and Pitard, Gilles and Le Goïc, Gaetan and Brost, Vincent and Mansouri, Alamin and Pamart, Anthony and Vallet, Jean-Marc and De Luca, Livio, A new method for calibration of the spatial distribution of light positions in free-form RTI acquisitions, Optics

for Arts, Architecture, and Archaeology VII, volume 11058, page 1105813, 2019, International Society for Optics and Photonics

[3] Karaszewski, Maciej and Adamczyk, Marcin and Sitnik, Robert, Assessment of next-best-view algorithms performance with various 3D scanners and manipulatorm, volume 119, pages 320-333,2016, ISPRS Journal of Photogrammetry and Remote Sensing, Elsevier

[4] Degrigny, Christian and Piqué, Francesca and Papiashvili, Nutsa and Guery, Julien and Mansouri, Alamin and Le Goïc, Gaëtan and Detalle, Vincent and Martos-Levif, Dominique and Mounier, Aurélie and Wefers, Stefanie and others, Technical study of Germolles' wall paintings: the input of imaging technique, Virtual Archaeology Review, volume 7, number 15, pages 1-8, 2016,Universitat Politècnica de València

[5] Nicodemus, Fred E, Directional reflectance and emissivity of an opaque surface, Journal of Applied optics, volume 4, number 7, pages 767-775,1965,Optical Society of America

[6] Wang, Oliver and Gunawardane, Prabath and Scher, Steve and Davis, James, Material classification using BRDF slices, pages 2805-2811, 2009, IEEE Conference on Computer Vision and Pattern Recognition

[7] Gautron, Pascal and Krivánek, Jaroslav and Pattanaik, Sumanta N and Bouatouch, Kadi, A Novel Hemispherical Basis for Accurate and Efficient Rendering,Rendering Techniques, volume 2004,page 321-330, 2004

[8] Pitard, Gilles and Le Goïc, Gaëtan and Mansouri, Alamin and Favrelière, Hugues and Desage, Simon-Frederic and Samper, Serge and Pillet, Maurice, Discrete Modal Decomposition: a new approach for the reflectance modeling and rendering of real surfaces, Machine Vision and Applications, volume 28, number 5, pages 607-621, 2017, Springer.

[9] Pintus, Ruggero and Dulecha, Tinsae Gebrechristos and Ciortan, Irina and Gobbetti, Enrico and Giachetti, Andrea, State-of-the-art in Multi-Light Image Collections for Surface Visualization and Analysis,Computer Graphics Forum, volume 38,number 3, pages 909-934,2019, Wiley Online Library

[10] Giachetti, Andrea and Ciortan, Irina and Daffara, Claudia and Pintus, Ruggero and Gobbetti, Enrico and others, Multispectral RTI analysis of heterogeneous artworks, The Eurographics Association, 2017

[11] Nurit, Marvin and Castro, Y and Zendagui, Abir and Le Goïc, Gaëtan and Favreliere, Hugues and Mansouri, Alamin, High dynamic range reflectance transformation imaging: an adaptive multi-light approach for visual surface quality assessment, Fourteenth International Conference on Quality Control by Artificial Vision, volume 11172, pages 1117213, 2019, International Society for Optics and Photonics

[12] Lemesle, Julie and Robache, Frederic and Le Goic, Gaetan and Mansouri, Alamin and Brown, Christopher A and Bigerelle, Maxence, Surface reflectance: An optical method for multiscale curvature characterization of wear on ceramic-metal composites,Materials Journal, volume 13, number 5, pages 1024, 2020, Multidisciplinary Digital Publishing Institute

[13] Coules, HE and Orrock, PJ and Seow, CE, Reflectance Transformation Imaging as a tool for engineering failure analysis,Journal of Engineering Failure Analysis, volume 105, pages 1006-1017, 2019, Elsevier

JOIN US AT THE NEXT EI!

IS&T International Symposium on

Electronic Imaging

SCIENCE AND TECHNOLOGY

Imaging across applications . . . Where industry and academia meet!

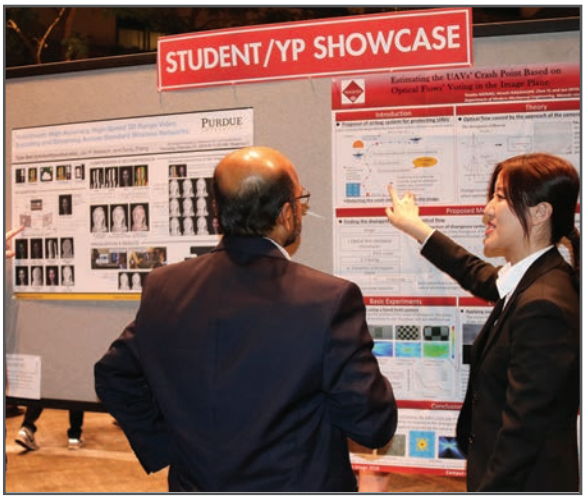

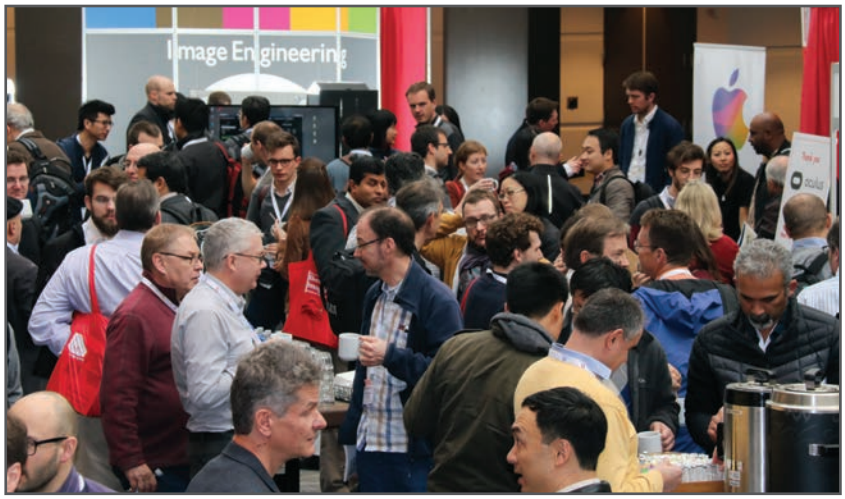

• SHORT COURSES • EXHIBITS • DEMONSTRATION SESSION • PLENARY TALKS •
• INTERACTIVE PAPER SESSION • SPECIAL EVENTS • TECHNICAL SESSIONS •

www.electronicimaging.org

IS&T
imaging.org